Journal of Alloys and Compounds 507 (2010) 53–61

Contents lists available at ScienceDirect

Journal of Alloys and Compounds

journal homepage: www.elsevier.com/locate/jallcom

Effect of microstructure on the quench sensitivity of AlZnMgCu alloys

Shengdan Liu[a,b,*], Wenjun Liu[a,b], Yong Zhang[a,b,c], Xinming Zhang[a,b], Yunlai Deng[a,b]

[a] School of Materials Science and Engineering, Central South University, Changsha 410083, China
[b] Key Laboratory of Nonferrous Materials, Ministry of Education, Central South University, Changsha 410083, China
[c] ARC Centre of Excellence for Design in Light Metals, Department of Materials Engineering, Monash University, Melbourne, Australia

ARTICLE INFO

Article history:
Received 14 July 2009
Received in revised form 14 July 2010
Accepted 15 July 2010
Available online 22 July 2010

Keywords:
7055 aluminum alloy
Microstructure
Quench sensitivity
Dispersoids
(Sub)grain boundaries

ABSTRACT

The effect of microstructure on the quench sensitivity of 7055 type aluminum alloys was investigated by hardness testing, optical microscopy and transmission electron microscopy. The results showed that the homogenized and hot-rolled alloys without Zr and the homogenized alloy with Zr were not quench sensitive, while the hot-rolled alloy with Zr was quite quench sensitive. The reason was analyzed according to the difference in the microstructure in these alloys, i.e. type of nucleation sites including dispersoids, (sub)grain boundaries and constituent particles for heterogeneous precipitation during slow quenching. Quench-induced η phase was observed mainly on large dispersoids and (sub)grain boundaries. In the homogenized and hot-rolled alloys without Zr, grain boundaries, which were the main heterogeneous precipitation nucleation sites, resulted in low quench sensitivity. In the homogenized alloy with Zr, grain boundaries and fine and coherent Al_3Zr dispersoids led to low quench sensitivity. In the hot-rolled alloy with Zr, the large number of coarse Al_3Zr dispersoids and subgrain boundaries were mainly responsible for high quench sensitivity. Constituent particles seemed to have little effect on quench sensitivity.

1. Introduction

AlZnMgCu alloys are widely used as structural materials in the aircraft industry due to their high specific strength. With the development of the aircraft industry, larger structural components with high properties are required. To meet the demand, products with large-gauge section such as thick plates of AlZnMgCu alloys are often desirable. The quench sensitivity of AlZnMgCu alloys is unfavorable for obtaining thick plates or large forgings with high properties because difference in the cooling rate between the surface and the mid-plane often results in heterogeneity and drop in properties. For instance, Robinson and Cudd [1] showed that in a 7010 aluminum alloy forging with size of 562(L) mm × 265(LT) mm × 169(ST) mm, the yield strength was 51 MPa higher at the corner than at the core location after aging. Moreover, in some cases slow quench is required to reduce distortion and residual stress [2], and this often gives rise to drop in mechanical properties after aging. Therefore, it is desirable to decrease the quench sensitivity. Many investigations have been performed on quench sensitivity of AlZnMgCu alloys due to their practical importance [3–11].

Quench sensitivity can be influenced by chemical compositions. For instance, higher amount of alloying elements often gives rise to higher quench sensitivity [3,4], and adjustment of Zn:Mg ratio may decrease quench sensitivity [4,5]. As for microstructure, it has been found that quench sensitivity is associated with nucleation sites, e.g. (sub)grain boundaries and dispersoids, available for heterogeneous precipitation during inadequate quench [6–9]. Dispersoids, determined by their nature, have great influence on quench sensitivity. For instance, zirconium instead of chromium has been added to AlZnMgCu alloys because Al_3Zr dispersoids are smaller and coherent, and lead to lower quench sensitivity [11]. Meanwhile, Al_3Zr dispersoids can control the grain structure effectively [12]. The coherent Al_3Zr dispersoids primarily precipitate during homogenization of ingot, and can survive during the following processing. Heterogeneous precipitation may occur on them due to the reduction of the misfit elastic energy [9]. Moreover, it has been found that Al_3Zr dispersoids may lose coherency with matrix due to recrystallization [13,14], consequently become effective heterogeneous nucleation sites for coarse equilibrium phase during slow quenching. As a result, quench sensitivity may be increased. Thus, if the microstructures in AlZnMgCu alloys are changed, the quench sensitivity may be changed accordingly.

7055 aluminum alloy has been developed to meet the requirement of improved aircraft structures, which demand a superior combination of high strength, good fracture toughness and good stress corrosion cracking resistance. These high properties can be achieved by T77 treatment, which is based on retrogression and reaging [15]. 7055–T77 alloy can offer higher strength about 10% than

* Corresponding author at: School of Materials Science and Engineering, Central South University, Changsha 410083, China. Tel.: +86 731 88830265; fax: +86 731 88830265.
E-mail address: csuliusd@163.com (S.D. Liu).

0925-8388/$ – see front matter © 2010 Elsevier B.V. All rights reserved.
doi:10.1016/j.jallcom.2010.07.124

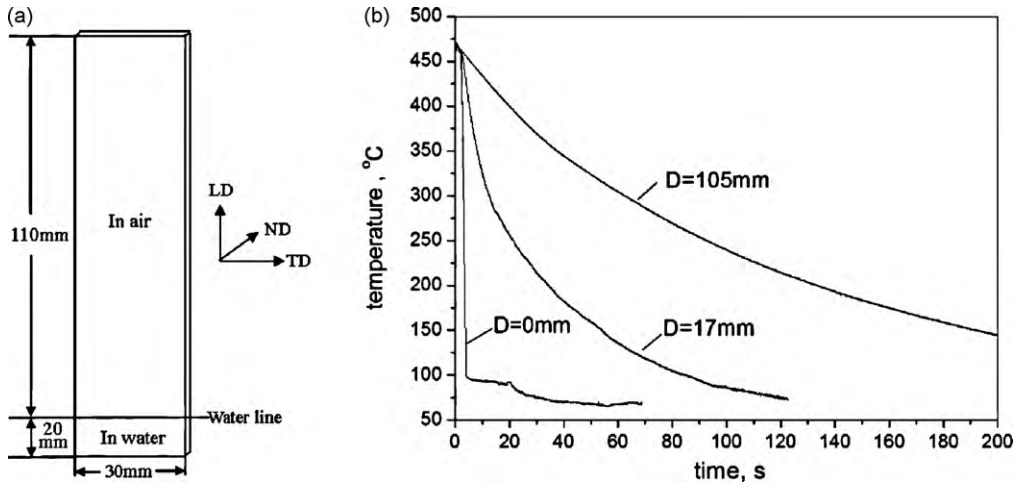

Fig. 1. (a) Schematic of the sample and quenching and (b) cooling curves at different positions along LD from the water line, LD: longitudinal direction, ND: normal direction, TD: transverse direction.

7150-T6 and 30% than 7075-T76 with high fracture toughness and good resistance to corrosion and to the growth of fatigue cracks, and these attractive properties are attributed to the high Zn/Mg and Cu/Mg ratios [16]. Due to the greater amount of (Zn + Mg + Cu) elements, this alloy is more quench sensitive than some other AlZn-MgCu alloys, as shown in a previous paper [17].

In this work, the effect of microstructure on quench sensitivity of 7055 type aluminum alloys with and without Zr was investigated with the aim to have better understanding of the quench sensitivity of AlZnMgCu alloys.

2. Experimental

Two 7055 type aluminum alloy ingots with nominal chemical compositions of Al–7.9Zn–2.2Mg–2.1Cu–0.15Zr (w.t.%) and Al–7.9Zn–2.2Mg–2.1Cu (w.t.%) were prepared. Al–5Ti-B alloy was used to refine the grains in the as-cast alloys and the content of Fe + Si was kept below 0.15%. The chemical compositions of AA7055 aluminum alloy are (w.t.%): Zn: 7.6–8.4, Mg: 1.8–2.3, Cu: 2.0–2.6, Zr: 0.08–0.25, Fe < 0.15, Si < 0.10. The content of the main alloying elements in the studied alloys was in the range of AA7055 Al alloy, but one had Zr and the other had no Zr. The two alloys were denoted as 7055–0.15Zr and 7055–0Zr respectively in the following sections. The ingots were homogenized by slowly heating to 465 °C, holding for 24 h and cooling in air. After pre-heating at 420 °C for 1 h, the homogenized ingots were rolled from 30 mm to 2.7 mm sheet with multi-passes. The homogenized ingots and rolled sheets were cut into rectangular samples with size of 2.7 mm × 30 mm × 130 mm. After solution heat treatment at 470 °C for 30 min, one end of the sample was cooled in room temperature water with the length of 20 mm in water, and other part of the sample was exposed to the still air, see Fig. 1(a). The cooling curve at different positions was measured by thermocouples attached to the sample by welding with results given in Fig. 1(b). According to Fig. 1(b), it is obvious that a decreasing quenching rate over the length of the sample was obtained, which was from about 170 °C/s at D = 0 mm to about 8 °C/s at D = 17 mm and to about 2 °C/s at D = 105 mm.The quenching rate was the average value calculated in the range of 420–230 °C, which is the critical temperature range for 7055 aluminum alloy [17]. After cooling to room temperature the samples were aged at 121 °C for 24 h immediately.

The Vickers hardness along the longitudinal direction (LD) of the aged sample was tested. A load of 5 kg was used and five measurements along transverse direction (TD) at each position D = 0–105 mm were made to obtain an average value. Samples for grain structure examination were ground, polished and etched by 10% H_3PO_4 solution, and then observed by Olympus PMG 3 optical microscopy (OM). The microstructures at D = 0 mm and 105 mm of the samples were further examined by Philips CM20 and Tecnai G^2 20 transmission electron microscopy (TEM) using 200 kV. And the LD–ND (normal direction) section was observed. For the hot-rolled samples, LD was the same as RD (rolling direction). Samples for TEM examination were ground to 0.2 mm, electro-chemically polished using solution of 70%CH_3OH + 30% H_3NO_3 below −20 °C. The average length of η′ hardening phase was estimated by measuring at least 100 precipitates from the image taken along ⟨0 1 1⟩ direction on TEM. The average width of grain boundary precipitate free zone (PFZ) was estimated by measuring at least five grain boundaries.

3. Results

3.1. Hardness curves

Fig. 2 shows hardness profiles of the studied alloys after aging. On the whole, the hardness decreases with quenching rate decreasing. For the homogenized alloys, there was only slight decrease in the hardness over the length regardless of Zr, see Fig. 2(a). At D = 105 mm, the drop percentage in the hardness was lower than 2%, which indicated very low quench sensitivity of the

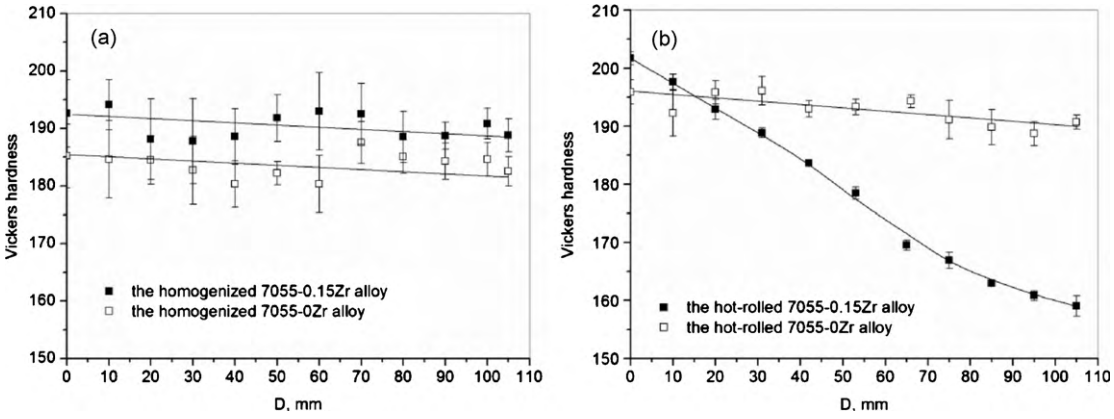

Fig. 2. Hardness profiles of the (a) homogenized and (b) hot-rolled alloys after solution heat treatment and aging.

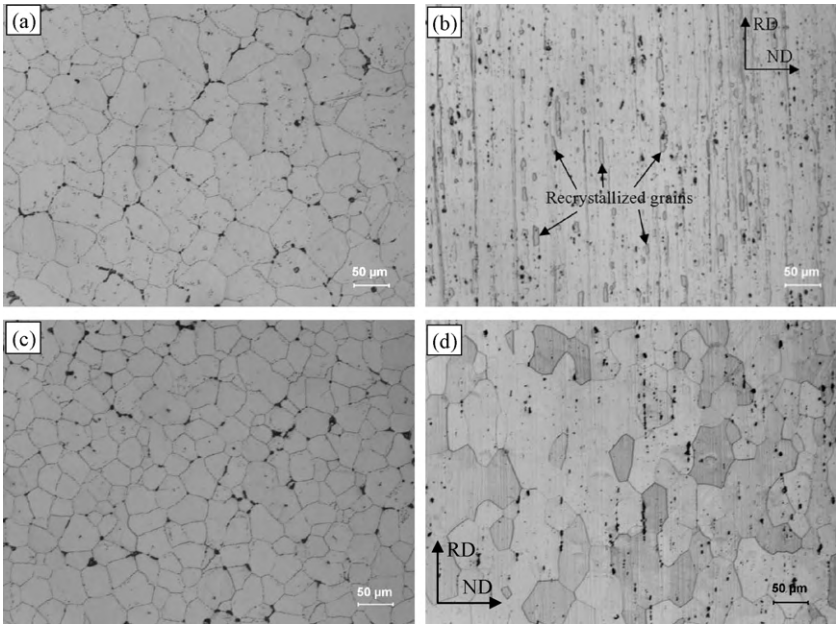

Fig. 3. Optical micrographs of the studied alloys after solution heat treatment: (a) the homogenized and (b) the hot-rolled 7055–0.15Zr alloy; (c) the homogenized and (d) the hot-rolled 7055–0Zr alloy.

homogenized alloys. From Fig. 2(b), it is evident that the hot-rolled 7055–0.15Zr alloy was quite quench sensitive because of significant drop in the hardness with distance away from the water line, and the drop percentage was about 21% at $D = 105$ mm. While the hot-rolled 7055–0Zr alloy was not quench sensitive, as the hardness decreased slightly with quenching rate decreasing, and the drop percentage in the hardness at $D = 105$ mm was about 2%.

It is evident that for 7055–0Zr alloy, the quench sensitivity was not changed by hot rolling, but for 7055–0.15Zr alloy, the quench sensitivity was increased greatly after hot rolling. This is supposed to be the difference in the microstructure due to hot rolling as the chemical compositions was not changed. The reason will be explored in detail in the following section.

3.2. Microstructure examination

3.2.1. Optical micrographs

Fig. 3 shows optical micrographs indicating the grain structure of the studied alloys. In the homogenized 7055–0.15Zr alloy, there were equiaxed grains, and the size (equivalent circle diameter) was about 50 μm. In the hot-rolled 7055–0.15Zr alloy, partial recrystallization occurred after solution heat treatment (Fig. 3(b)), which is obviously attributed to the recrystallization inhibiting effect of Al_3Zr dispersoids [8,9]. The recrystallization fraction was very low and estimated to be about 4%. The recrystallized grains were rod-like in the RD–ND section, and the average size was about 22 μm (along RD) × 6 μm (along ND). In the homogenized 7055–0Zr alloy, the grains were equiaxed with size about 42 μm; in the hot-rolled alloy, complete recrystallization occurred after solution heat treatment, the grain size was about 47 μm. In addition, some black second phase particles, which were mainly made up of Fe/Si-containing phase and Al_2CuMg phase, can be observed to be located at grain boundaries in the homogenized samples. After hot rolling, they were distributed along rolling direction.

3.2.2. Transmission electron micrographs

For the 7055–0Zr alloy, the quench sensitivity was not changed by hot rolling, so only the hot-rolled samples were selected for TEM examination, typical images are shown in Fig. 4. A significant change due to slow quenching is that the width of grain boundary precipitates free zone (PFZ) was increased from about 18.8 ± 3.8 nm at $D = 0$ mm to about 68.2 ± 27.5 nm at $D = 105$ nm. Moreover, the η′ hardening precipitates adjacent to the grain boundary was larger, and the density was lower. While in the matrix far from the grain boundaries, there were high density of η′ hardening precipitates. And occasionally, coarse η phase particles could be observed inside grains at $D = 105$ mm, see Fig. 4(c). Most of them were long-lath-shaped and their size was not uniform, the average size was about 137 nm in length and 34 nm in width.

For the 7055–0.15Zr alloy, the quench sensitivity was significantly increased by hot rolling, so both the homogenized and the hot-rolled samples were selected for TEM examination. Fig. 5 shows TEM micrographs of the homogenized sample after aging. At $D = 0$ mm (Fig. 5(a)), the matrix was primarily covered with a number of fine and dispersed η′ hardening precipitates. Observed along ⟨0 1 1⟩ direction, the η′ hardening precipitates were needle-shaped. At $D = 105$ mm, Al_3Zr dispersoids, η′ hardening precipitates and η phase could be identified in the matrix according to Fig. 5(b) and (c). The η phase particles were lath-shaped and associated with Al_3Zr dispersoids as indicated by the arrows in Fig. 5(b), and the average size was about 25 nm in length and 6 nm in width. The length of needle-shaped η′ hardening precipitates inside grains at $D = 0$ mm and 105 mm was almost the same (Table 1). The precipitation at the grain boundaries in the materials at the two positions was different, see Fig. 6. At $D = 0$ mm, η phase particles were distributed continuously along most grain boundaries (Fig. 6(a)), and the precipitates free zone(PFZ) was quite narrow with the width of about 21.7 ± 3.5 nm. While at $D = 105$ mm, η phase particles at most grain boundaries became more spaced, and the size was not uniform. The width of the PFZ near grain boundaries was obviously larger and about 64.1 ± 27.3 nm (Fig. 6(b)). It could also be found that η′ hardening precipitates adjacent to the grain boundaries were slightly larger than those in the matrix far from the grain boundaries.

At $D = 0$ mm in the hot-rolled 7055–0.15Zr alloy after solution heat treatment and aging, the matrix was covered by high density of fine η′ hardening precipitates, as indicated by typical TEM image and corresponding ⟨0 1 1⟩ selected area diffraction pattern (SADP) in Fig. 7(a) and (b). The needle-shaped η′ precipitates were distributed uniformly in the grains, and the length was estimated to be about 4.7 nm. At $D = 105$ mm, the microstructure was quite complex

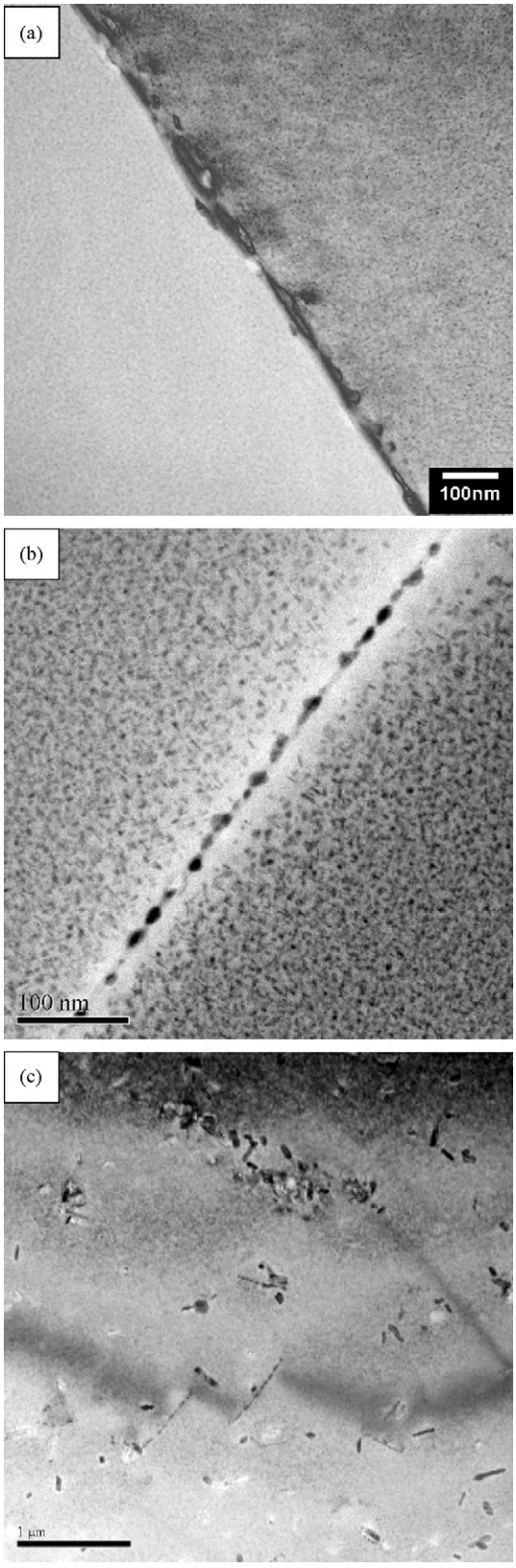

Fig. 4. TEM images of the hot-rolled 7055–0Zr alloy after solution heat treatment and aging: (a) grain boundary at $D = 0$ mm; (b) grain boundary at $D = 105$ mm; and (c) inside a grain at $D = 105$ mm.

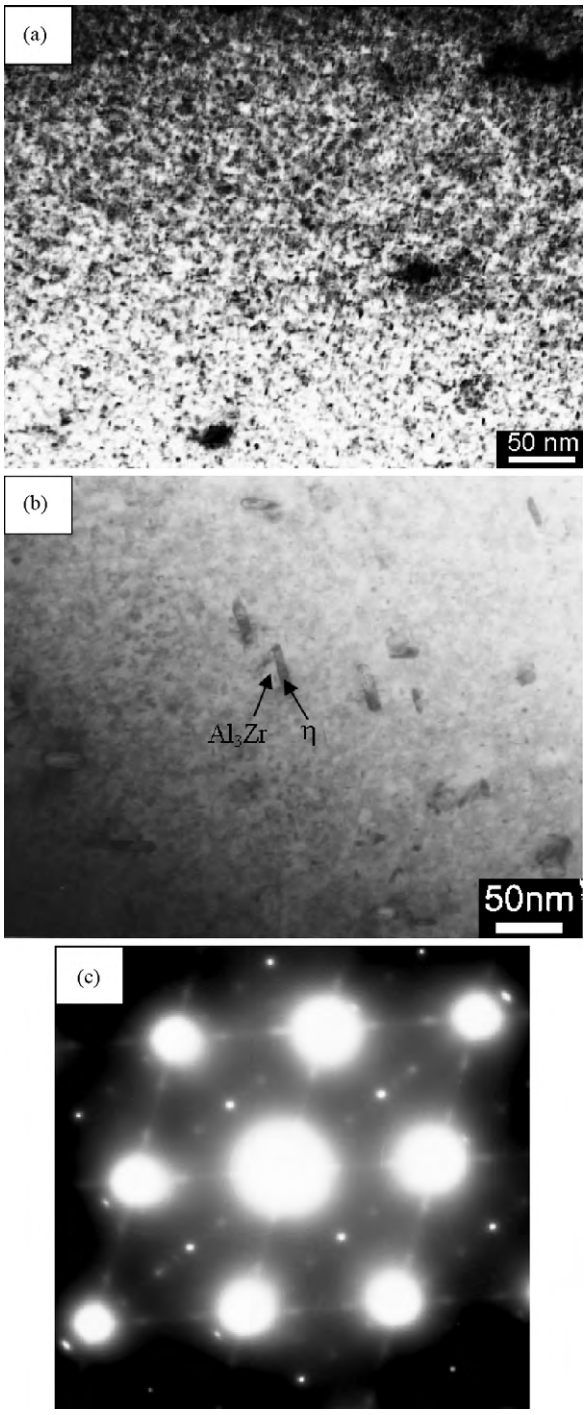

Fig. 5. TEM images of the homogenized 7055–0.15Zr alloy after solution heat treatment and aging: (a) $D = 0$ mm; (b) $D = 105$ mm; and (c) corresponding ⟨0 1 1⟩ SAD pattern from (b).

because of partial recrystallization (Fig. 3(b)), and typical TEM images are shown in Fig. 8. In the recrystallized grains (Fig. 8(a)), there were a number of quench-induced η phase particles distributed in bands along the rolling direction and in layers along normal direction. Most of these η phase particles had the shape of long lath with average size of about 210 nm (in length) × 35 nm(in width). An obvious precipitates free zone formed around these particles, see Fig. 8(b). Though there were still some η′ hardening precipitates in the band of these particles, the density is significantly lower and the size is larger compared with the η′ precipitates in the matrix far from these large particles (Table 1). It was also

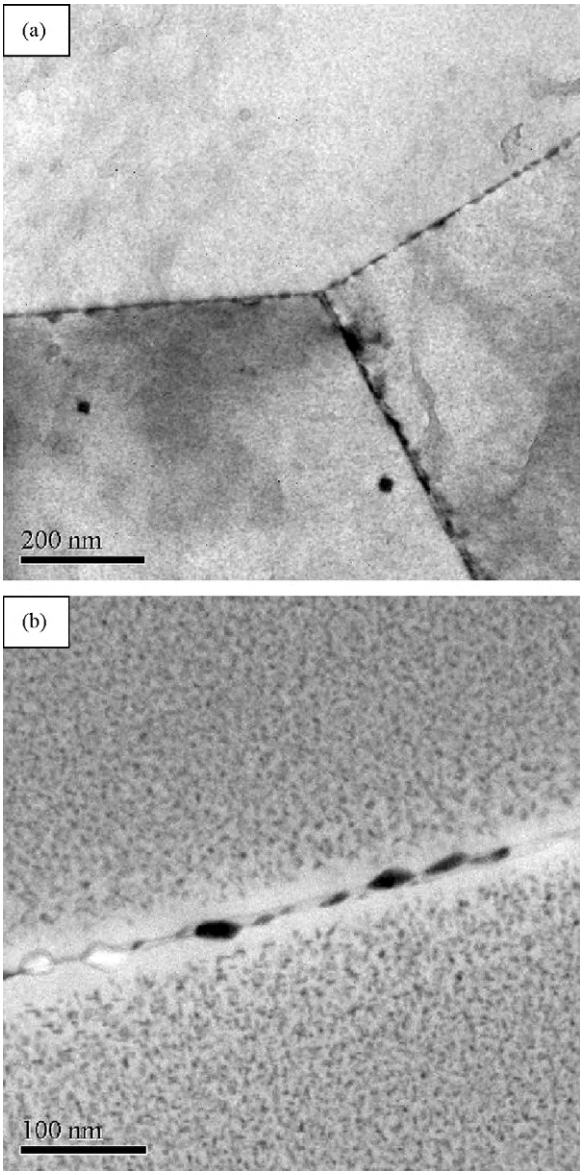

Fig. 6. TEM images of precipitation at grain boundaries in the homogenized 7055–0.15Zr alloy: (a) $D = 0$ mm and (b) $D = 105$ mm.

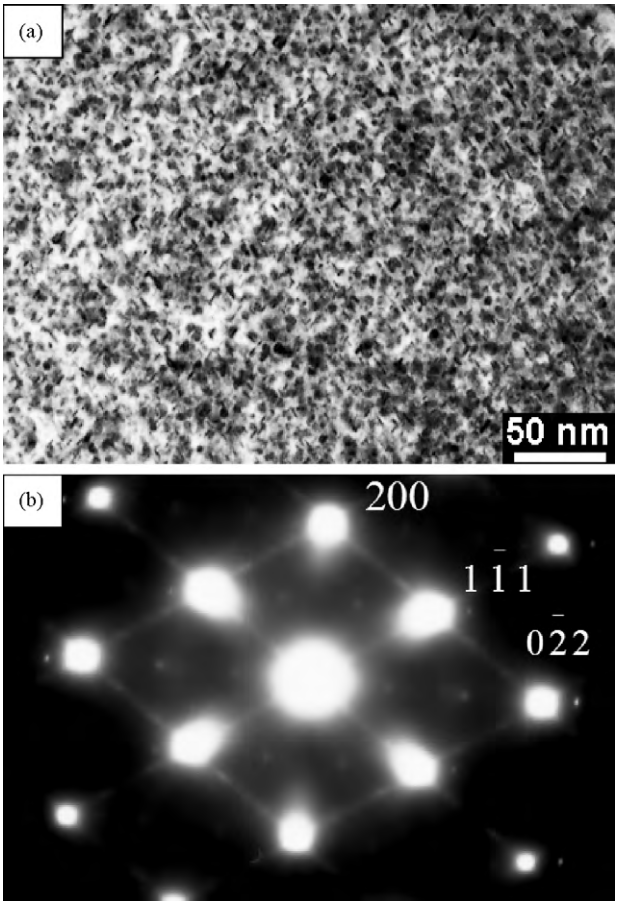

Fig. 7. TEM image of the hot-rolled 7055–0.15Zr alloy at $D = 0$ mm after solution heat treatment and aging: (a) morphology of hardening precipitates and (b) corresponding ⟨0 1 1⟩ SAD pattern.

found that most η phase particles were associated with Al_3Zr dispersoids. A close look at the center layer of the recrystallized grain indicated a lot of Al_3Zr dispersoids unoccupied by quench-induced η phase (Fig. 8(c)). These Al_3Zr dispersoids were coherent with the Al matrix according to the distinct no-contrast lines [15]. In the unrecrystallized zone, there were many well defined subgrains, but their size was not uniform, typical image is shown in Fig. 8(a). It can be seen that some subgrains were quite small with size less than 1 μm, while others were larger with size about 1–3 μm. In the area with small subgrains, some coarse η phase particles could be observed at subgrain boundaries but few inside subgrains. While in the area with large subgrains, coarse η phase particles could be observed both inside subgrains and at subgrain boundaries, see Fig. 8(d). The η phase particles inside subgrains were quite large and often had the shape of long lath with the average size of about 150 nm (in length) × 30 nm (in width). In a previous paper, it was suggested that once particles nucleated on dispersoids, they grew to a similar size regardless of alloy or quench rates [3]. In this work, it has been found that the quench-induced phase in the homogenized 7055–0.15Zr alloy was significantly smaller than that in the hot-rolled 7055–0.15Zr alloy as shown in Table 1. It is supposed that apart from the capability of Al_3Zr dispersoids to stimulate nucleation, larger amount of residual dislocations introduced by hot rolling may contribute to larger quench-induced phase.

Another difference in the microstructure due to slow quenching could be observed at grain boundaries, typical TEM images are shown in Fig. 9. At $D = 0$ mm, it seems that most grain boundaries were decorated with closely spaced η phase particles and the PFZ was narrow with average width about 17.5 ± 1.7 nm (Fig. 9(a)). While at $D = 105$ mm, big difference can be seen in the size of η phase particles at (sub)grain boundaries. Many small η phase particles could be found between large η phase particles, as shown in Figs. 8(d) and 9(b). The large η phase particles were about 150 nm in length along the grain boundary, while the small ones were about 20 nm. It is supposed that the large η phase particles were formed during slow quenching and grew during subsequent artificial aging. The small ones were formed during artificial aging. Another phenomenon is that the width of PFZ near grain boundary was different at different positions. At the position where the quench-induced η phase stays (e.g. Fig. 9(b)), the PFZ is about 86.4 ± 10.3 nm in width; while near the aging-induced η phase particles, the PFZ was about 51.3 ± 5.6 nm in width. Moreover, larger η′ hardening precipitates were observed near the grain boundary than inside grain far from the grain boundary, which is similar to that found in the homogenized 7055–0.15Zr alloy (Fig. 6) and the hot-rolled 7055–0Zr alloy after slow quenching (Fig. 4).

Table 1
Average size of η′ and η phase in the aged alloys.

Sample	Length of needle-shaped η′ precipitates (nm)		Size of quench-induced lath-shaped η phase at D = 105 mm (length × width nm)
	D = 0 mm	D = 105 mm	
Homogenized 7055–0.15Zr alloy	5.2 ± 1.1	5.7 ± 0.9	25 × 6
Hot-rolled 7055–0.15Zr alloy	4.7 ± 1.2	4.9 ± 1.3 (in the matrix) 15.6 ± 3.2 (in η band)	210 × 35 (in REX grains[a]) 150 × 30 (in subgrains)
Hot-rolled 7055–0Zr alloy	5.9 ± 1.4	5.6 ± 1.2	137 × 34

[a] REX grains: recrystallized grains.

Table 2
Possible heterogeneous precipitation sites in the studied alloys during slow quenching.

Alloy	Possible nucleation sites for heterogeneous precipitation
Homogenized 7055–0Zr alloy	Grain boundaries, constituent particles
Hot-rolled 7055–0Zr alloy	Grain boundaries, constituent particles
Homogenized 7055–0.15Zr alloy	Grain boundaries, Al_3Zr dispersoids, constituent particles
Hot-rolled 7055–0.15Zr alloy	Grain boundaries, subgrain boundaries, Al_3Zr dispersoids, constituent particles

4. Discussion

For Al–Zn–Mg–Cu alloys, large equilibrium phase formed during slow quenching results in loss of solutes, thus fewer η′ hardening precipitates after aging. The precipitation of equilibrium η phase is a nucleation and growth process [7] and may be greatly influenced by the number and type of sites that can prompt nucleation, or dislocations that can prompt growth. It is supposed that the quench sensitivity is closely related to the microstructure, i.e., the type and number of heterogeneous precipitation sites in the alloy. The hot-rolled 7055–0.15Zr alloy exhibited significantly higher quench sensitivity than other alloys because of difference in the microstructure. According to microstructure observations, the possible heterogeneous precipitation sites in each alloy are given in Table 2.

4.1. Effect of Al_3Zr dispersoids on quench sensitivity

From above results, it is evident that introducing Al_3Zr dispersoids had little effect on the quench sensitivity of the homogenized alloys. This may be due to the fact that most Al_3Zr dispersoids in the homogenized 7055–0.15Zr alloy were small and coherent with the matrix, as shown in Fig. 10(a). But the size of these Al_3Zr dispersoids was not uniform according to the dark field image in Fig. 10(b). Large dispersoids can stimulate nucleation of η phase more efficiently during slow quenching [7,18], which is due to a partial loss of coherency for these dispersoids. In this work, some η phase particles on dispersoids were observed in the homogenized 7055–0.15Zr alloy after slow quenching, but these particles were quite small (Fig. 5, Table 1), and seemed to have exerted little influence on the precipitation microstructure in the matrix around them. Thus, only slight drop (≈2%) in the hardness was observed (Fig. 2), and the homogenized 7055–0.15Zr alloy was not quench sensitive.

In the hot-rolled 7055–0.15Zr alloy, Al_3Zr dispersoids are still the possible nucleation sites for heterogeneous precipitation in the matrix during slow quenching. But the situation is more complex due to partial recrystallization after solution heat treatment. According to TEM observation (Fig. 8(a)), the quench-induced η phase particles exhibited bands distribution along RD and layered-distribution along ND in the recrystallized grain. This is obviously associated with the spatial distribution pattern of Al_3Zr dispersoids after hot rolling, see Fig. 11(a). In Al–Zn–Mg–Cu–Zr alloys, an inhomogeneous distribution of Zr often exists [19]. Moreover, the diffusivity of Zr in Al is very low. Thus, long thin bands distribution of Al_3Zr dispersoids can be obtained after rolling and solution heat treatment, which is similar to the observation in Deschamps' study [9]. The distribution of η phase particles formed during slow quenching exhibited the same pattern as shown in Fig. 8(a). It has been found that due to recrystallization, Al_3Zr dispersoids may lose coherency with the matrix and become effective nucleation sites for heterogeneous precipitation [14]. However, as shown in Fig. 8(c), there were a number of coherent Al_3Zr dispersoids inside the recrystallized grain, and they were not occupied by coarse η phase particles. It is evident that recrystallization resulted in preferential coarsening and gradual loss of coherency of some Al_3Zr dispersoids. Thus, the density of η phase particles was different at different positions. In the area with small and coherent Al_3Zr dispersoids, low density of η phase particles can be seen (B1 in Fig. 8(a)); while in the area with large and incoherent Al_3Zr dispersoids, higher density of η phase particles can be seen (B2 in Fig. 8(a)). The matrix in the coarse η phase bands, as expected, was almost free of fine hardening precipitates, because the solute-depleted zone due to slow quenching can inhibit precipitation during aging [9]. And if there were precipitates, the size was significantly larger (Fig. 8(b)). Thus, these zones were soft for lack of fine precipitates. The precipitation microstructure in the matrix far from the coarse η phase bands was unaffected by heterogeneous precipitation and covered with high density of fine η′ precipitates. This kind of microstructure may be one reason for lower hardness after aging, as shown in Fig. 2.

In the unrecrystallized zone, it is thought that the situation is similar to that in the homogenized 7055–0.15Zr sample. The Al_3Zr dispersoids may act as heterogeneous nucleation sites determined by their size and coherency. During solution heat treatment at high temperature, significant coarsening of some Al_3Zr dispersoids occurs due to a large number of dislocations introduced by rolling. As a result, the size of Al_3Zr dispersoids in the subgrains was not uniform (Fig. 11(b)), and some even were coarsened to be about 100 nm (indicated by A in Fig. 11(c)). Coarse dispersoids are less coherent or incoherent with the matrix due to their larger size [20]. This may increase their nucleation efficiency for heterogeneous precipitation. Thus η phase can form on the large dispersoids during slow quenching. Inside small subgrains (Fig. 8(a)), few quench-induced η phase particles were observed, which may be because Al_3Zr dispersoids are small and coherent with matrix. While in large subgrains, some coarse quench-induced η phase particles associated with dispersoids were detected in the matrix (Figs. 8(a), (d) and 11(c)). The dispersoids A is large and incoherent with the matrix, while others are small and coherent with the matrix according to the no-contrast lines.

In all, small and coherent dispersoids do not lead to high quench sensitivity, which is the case for the homogenized 7055–0.15Zr alloy (Fig. 2(a)), but large and incoherent dispersoids can lead to

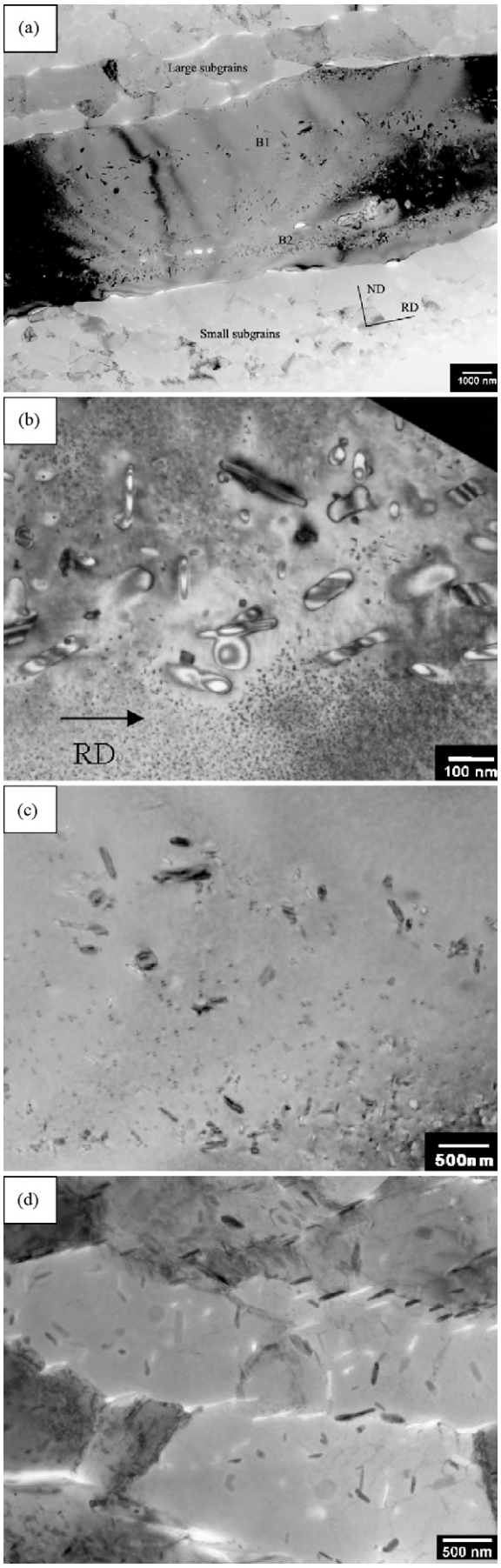

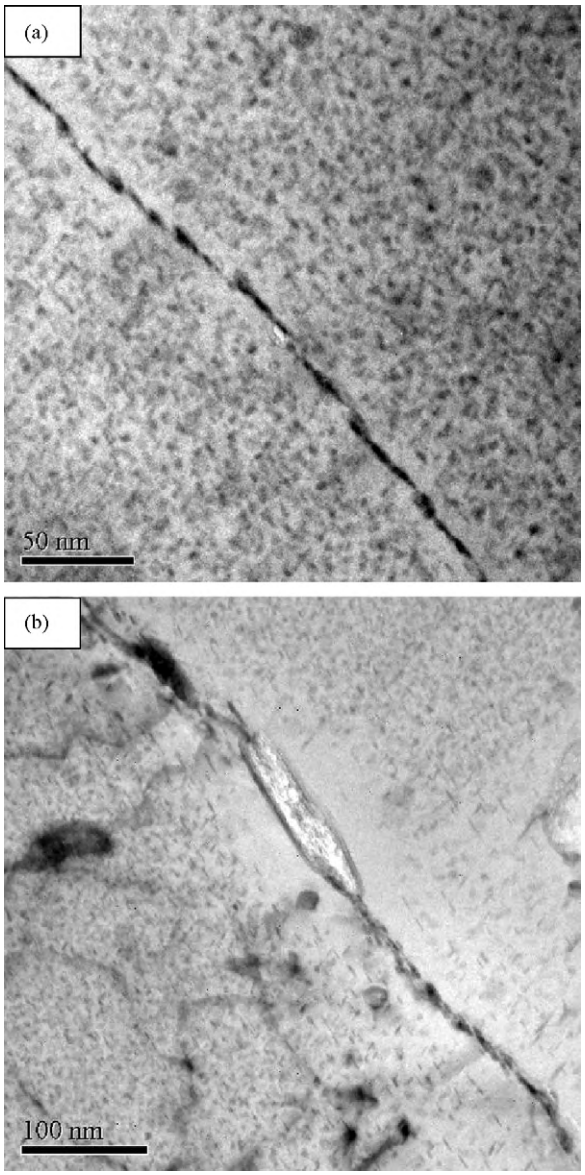

Fig. 9. TEM images of precipitation at grain boundaries in the hot-rolled 7055–0.15Zr alloy after solution heat treatment and aging: (a) $D = 0$ mm and (b) $D = 105$ mm.

high quench sensitivity as shown by 7055–0.15Zr alloy after hot rolling (Fig. 2(b)). Whether there is a critical size that Al_3Zr dispersoids must exceed to be able to act as heterogeneous nucleation site is unknown. But there exists a critical size for the coherent dispersoids to transform into semi-coherent or incoherent dispersoids [21]. And this is a quite complicated problem, because many parameters, e.g. chemical compositions, processing history, can exert influence on the coarsening kinetics of Al_3Zr dispersoids. Deformation may accelerate the growth of Al_3Zr dispersoids by introducing a lot of dislocations. Zn, Mg and Cu atoms may enter Al_3Zr dispersoids [22], thus have influence on the stability. Further investigations are still required to contribute to understanding of this problem.

Fig. 8. TEM images of the hot-rolled 7055–0.15Zr alloy at $D = 105$ mm after solution heat treatment and aging: (a) low magnification; (b) precipitates in the recrystallized grain; (c) dispersoids and coarse η phase inside the recrystallized grain; and (d) coarse η phase in the large subgrains zone, ND: normal direction, RD: rolling direction.

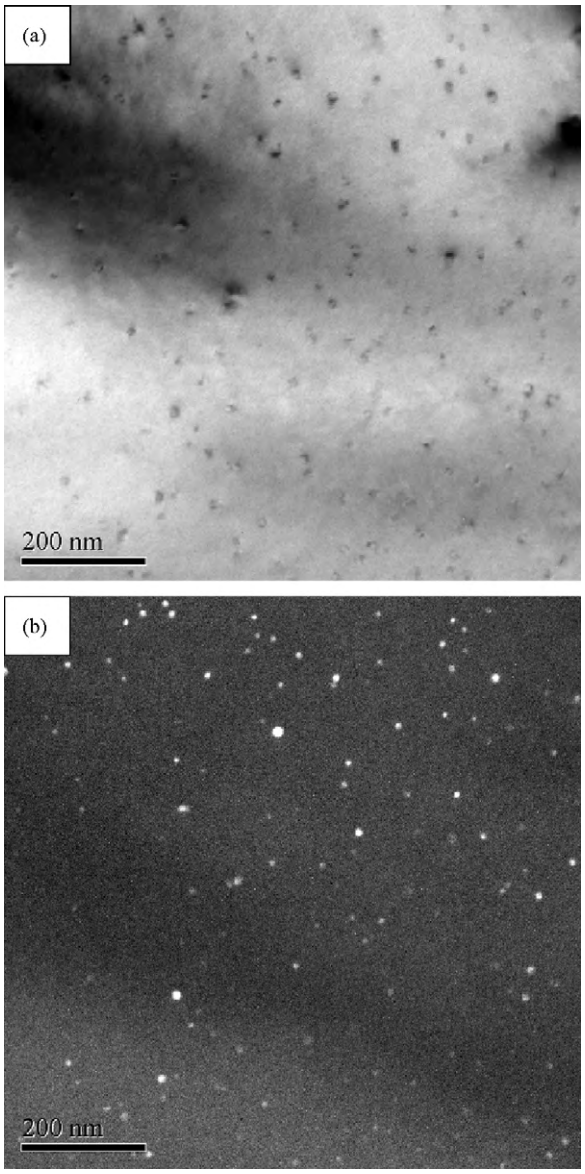

Fig. 10. TEM images showing the Al_3Zr dispersoids in the homogenized 7055–0.15Zr alloy after solution heat treatment and rapid quenching: (a) bright field image and (b) dark field image.

4.2. Effect of (sub)grain boundaries on quench sensitivity

During slow quenching, there is a strong tendency for precipitation to occur at grain boundaries and subgrain boundaries due to their high interfacial energy. Preferential precipitation at (sub)grain boundaries during slow quenching resulted in η phase particles of non-uniform size along (sub)grain boundaries after aging [8]. Moreover, loss of solutes and vacancies adjacent to (sub)grain boundaries gives rise to wider PFZ and larger η′ hardening precipitates(e.g. Fig. 4). But this change due to slow quenching is limited to the grain boundary zone, and not observed inside grains far from grain boundaries. This kind of microstructure results in only slight drop in the strength of a wrought AlZnMgCu alloy without Zr after delayed quench, as shown in a previous paper [23]. In the homogenized and hot-rolled 7055–0Zr alloys and the homogenized 7055–0.15Zr alloy, the grains are large and the size is similar, thus, the quench sensitivity is low and the drop in the hardness due to slow quenching is similar (Fig. 2). But when a large number of subgrain boundaries is introduced, the quench sensitivity seems to have been increased. The more subgrain boundaries,

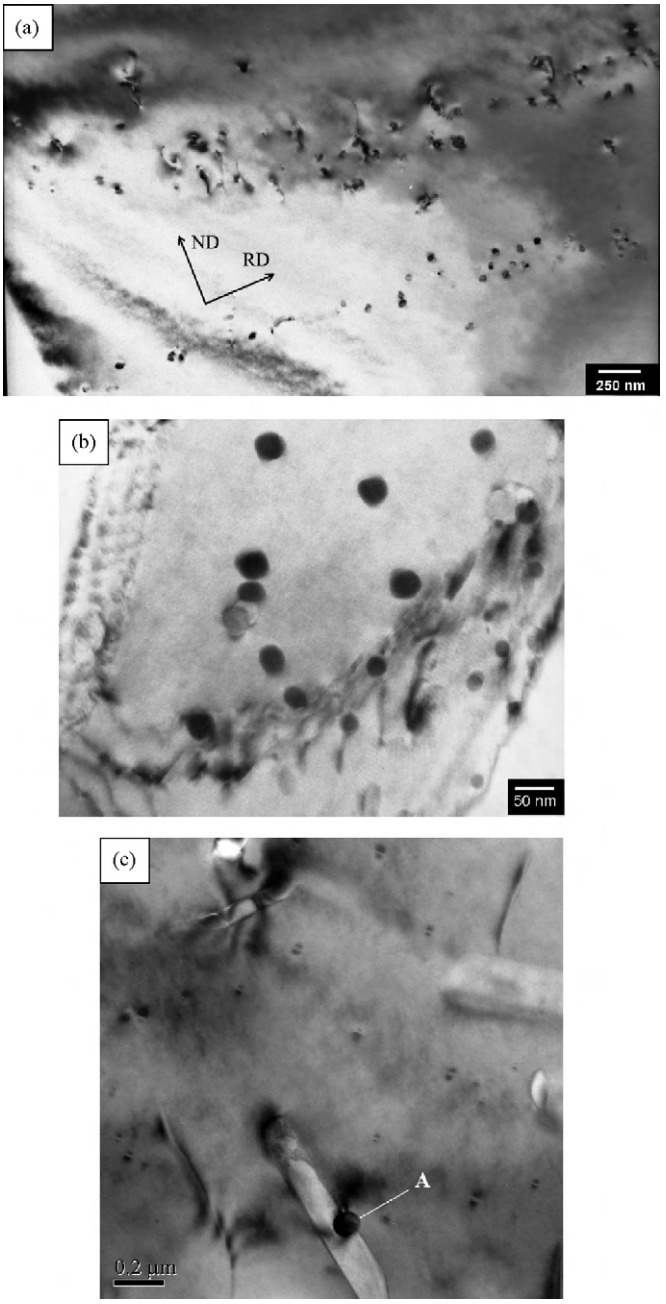

Fig. 11. TEM images showing the microstructure in the hot-rolled 7055–0.15Zr alloy after solution heat treatment and quenching, $D = 0$ mm: (a) in a recrystallized grain and (b) in a subgrain; $D = 105$ mm: (c) in a subgrain.

the more quench-induced equilibrium phase. Thus, the amount of solutes available for η′ hardening precipitates is reduced. Simultaneously, the amount of larger η′ hardening precipitates near subgrain boundaries (Fig. 9(b)) is increased. This means fewer fine and dispersed η′ hardening precipitates were attained. Consequently, lower strengthening effect can be achieved after aging. This is supposed to be partly responsible for the high quench sensitivity of the hot-rolled 7055–0.15Zr alloy.

4.3. Effect of constituent particles on quench sensitivity

Apart from dispersoids and (sub)grain boundaries, constituent particles can be observed in the studied alloys after solution heat treatment. This may have influence on the quench sensitiv-

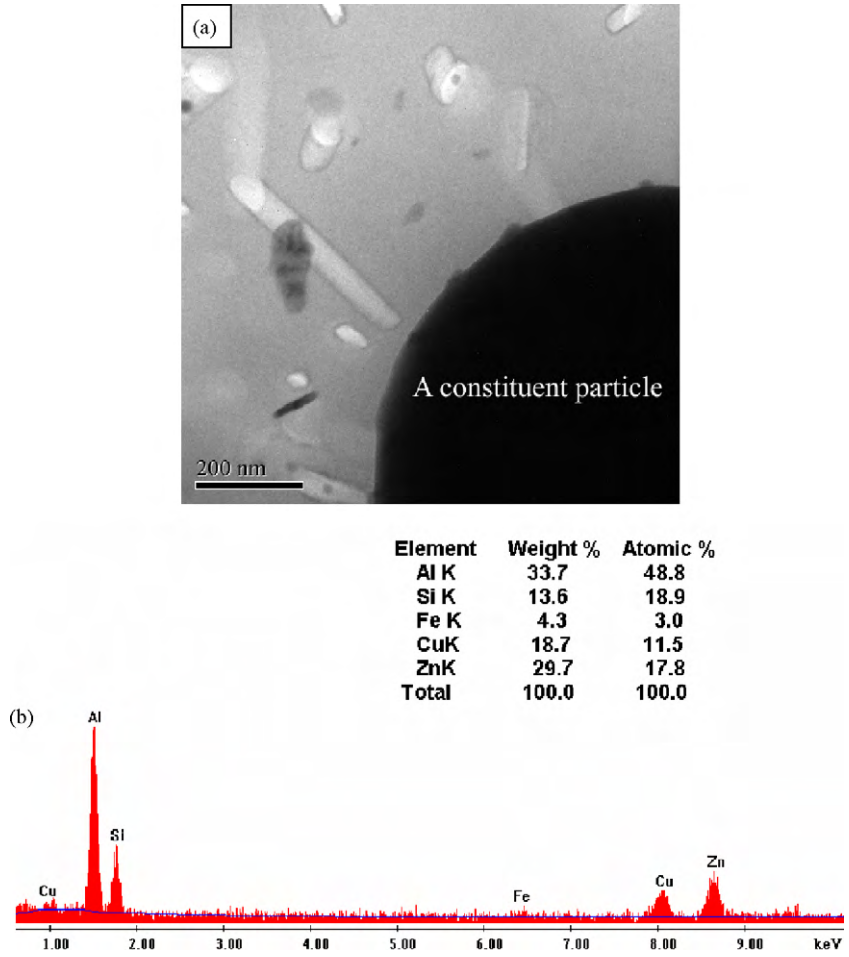

Fig. 12. A constituent particle in the hot-rolled 7055–0.15Zr alloy after solution heat treatment and slow quenching: (a) morphology and (b) EDS results.

ity because the interface between the constituent particles and the matrix may provide nucleation sites for heterogeneous precipitation. But few quench-induced η phase particles have been observed on the constituent particles, typical observation is shown in Fig. 12(a). The globule constituent particle contained impurity elements Fe and Si from the EDS results in Fig. 12(b). It is supposed that under the cooling condition in this work the constituent particles did not act as the heterogeneous precipitation nucleation sites, thus had little effect on quench sensitivity.

5. Conclusions

Heterogeneous precipitation occurred at grain boundaries, subgrain boundaries and on large Al_3Zr dispersoids during slow quenching. The existence of grain boundaries in the homogenized and hot-rolled 7055 type Al alloys without Zr results in low quench sensitivity. Grain boundaries and fine and coherent Al_3Zr dispersoids in the homogenized 7055 Al alloy led to low quench sensitivity. The large number of subgrain boundaries and Al_3Zr dispersoids with large size was responsible for the high quench sensitivity of the hot-rolled 7055 Al alloy. Constituent particles may have little effect on quench sensitivity because of few quench-induced η phase particles on the interface.

Acknowledgements

The authors are grateful to the help for microstructure examination provided by Mr. Muddle (B.C. Muddle) and Mr. Gao (S. Gao) from Monash University, Melbourne, Australia. The authors would like to thank anonymous reviewer for his advice. And the financial support from the Key Fundamental Research Project of China (2005CB623700) and the Freedom Explore Program of Central South University (201012200238) is also acknowledged.

References

[1] J.S. Robinson, R.L. Cudd, J. Mater. Process. Technol. 119 (2001) 261.
[2] C.E. Bates, G.E. Totten, Heat Treat. Met. 4 (1988) 89.
[3] D. Dumont, A. Deschamps, Y. Bréchet, Mater. Sci. Technol. 20 (2004) 567.
[4] S.D. Liu, Q.M. Zhong, Y. Zhang, Mater. Des. 31 (2010) 3116.
[5] S.T. Lim, S.J. Yun, S.W. Nam, Mater. Sci. Eng. A 371 (2004) 82.
[6] A. Deschamps, C. Bréchet, Scripta Mater. 39 (1998) 1517.
[7] D. Godard, P. Archambault, E. Aeby-Gautier, Acta Mater. 50 (2002) 2319.
[8] S.D. Liu, X.M. Zhang, M.A. Chen, Mater. Charact. 59 (2008) 53.
[9] A. Deschamps, Y. Bréchet, Mater. Sci. Eng. A 251 (1998) 200.
[10] R.C. Dorward, D.J. Beerntsen, Metall. Mater. Trans. A 26 (1995) 2481.
[11] D.S. Thompson, B.S. Subramanya, S.A. Levy, Metall. Trans. 2 (1971) 1149.
[12] J.D. Robson, P.B. Prangnell, Mater. Sci. Technol. 18 (2002) 607.
[13] M. Kanno, B.L. Ou, Mater. Trans. 32 (1991) 445.
[14] S. Kikuchi, H. Yamazaki, T. Otsuka, J. Mater. Process. Technol. 38 (1993) 689.
[15] D.A. Lukasak, R.M. Hart, Aerospace Eng. 9 (1994) 21.
[16] J.E. Starke, J.T. Staley, Prog. Aerospace Sci. 32 (1996) 131.
[17] S.D. Liu, X.M. Zhang, J.H. You, Mater. Sci. Technol. 24 (2008) 1419.
[18] J.D. Robson, Mater. Sci. Eng. A 382 (2004) 112.
[19] J.D. Robson, P.B. Prangnell, Acta Mater. 49 (2001) 599.
[20] K.E. Knipling, D.C. Dunand, D.N. Seidman, Acta Mater. 56 (2008) 1147.
[21] S. Iwamura, Y. Miura, Acta Mater. 52 (2004) 591.
[22] G. Sha, A. Cerezo, Ultramicroscopy 102 (2005) 151.
[23] J.H. You, S.D. Liu, X.M. Zhang, J. Cent. South Univ. Technol. 15 (2008) 147.